



ASSESSMENT OF CENTENNIAL (1918 – 2019) DROUGHT FEATURES IN THE CAMPANIA REGION BY HISTORICAL IN SITU MEASUREMENTS

5 Antonia Longobardi¹, Ouafik Boulariah¹, Paolo Villani¹

¹Civil Engineering Department, University of Salerno, Fisciano, 84084, Italy

Correspondence to: Antonia Longobardi (alongobardi@unisa.it)



10 Abstract

Drought is a sustained period of below-normal water availability. It is a recurring and worldwide phenomenon, but the Mediterranean basin is seen as a very vulnerable environment in this perspective and understanding historical drought conditions in this area is necessary to plan mitigation strategies to further face future climate change impacts. The reported research was aimed at the description of drought conditions and evolution for the Campania region (Southern Italy), assessed
15 by the analysis of an in-situ measurement database which covers a centennial period from 1918-2019. SPI time series were reconstructed for different accumulation time scales (from 3 to 48 months) and the Modified Man Kendall and Sen's test were applied to identify SPI changes over time. SPI time series were mostly affected by a negative trend, significant for a very large area of the region, particularly evident for the accumulation scales larger than 12 months. Mean drought duration (MDD), severity (MDS) and peak (MDP) were furthermore investigated for both moderate ($SPI \leq -1$) and extremely severe conditions
20 ($SPI \leq -2$). The accumulation scale affected the drought features, with longer duration and larger severity associated to the larger accumulation scales. Drought characteristics spatial patterns were not congruent for the different SPI time scales: if duration and severity were larger in the southern areas, peaks appeared mostly severe in the northern areas of the region. Extremely severe events were featured by lower durations and larger severity compared to the moderate drought events but were very less frequent (over 75% less then) and did not appeared to be focused on specific areas of the region.

25



1 Introduction

Drought is a natural local or regional disaster which affects agricultural, hydrological, socio-economic, groundwater systems (Dracup et al., 1980; Mishra and Singh, 2010; Wilhite and Glantz, 1985). The climate change is likely to accelerate the climate-meteo-hydrological processes able to lead toward intense drought episodes in specific environments (Longobardi and Van Loon, 2018) and, in this perspective, in recent years and in several world regions, the drought evolution has been widely discussed and analyzed.

In different areas of Asia, the spatio-temporal variability of drought has been discussed by Zhang and Zhou (2015) and by Hasegawa et al. (2016). In America, regional drought events have been reviewed by Swain and Hayhoe (2015), Littell et al. (2016) and Sobral et al. (2019). Spinoni et al. (2015) and Stagge et al. (2017) analyzed drought events in different region of Europe. In particular for this specific geographical context, according to the IPCC fifth Assessment Report (AR5), the Mediterranean basin is seen as a very vulnerable environment (Change, 2014) and a number of regional scale drought analyses have been indeed performed in different regions of this area (Cook et al., 2016; Gouveia et al., 2017; Ruffault et al., 2018; Caloiero et al., 2019; Yves et al., 2020). At the global scale, south America, the Sahel, the Congo River Basin and the north-eastern China, besides the Mediterranean basin, resulted as the areas most frequently affected by severe droughts (Spinoni et al., 2019).

The Italian territory is vulnerable to drought episodes and the lack of reliable climate data makes difficult temporal and spatial evaluation at a spatial resolution adequate to the interpretation of the effects associated to the precipitation scarcity. Coarse spatial resolution data from global weather dataset are poorly effective because of the high precipitation variability that affects the southern Europe regions indeed, thus historical in-situ long term measurements are crucial for understanding historical drought conditions and to plan mitigation strategies to face future climate change impacts (Bonaccorso and Aronica, 2016; Marini et al., 2019).

One of the widely used approach to define drought conditions and persistence consists in the use of mathematical indices, known as drought indicators, such as the Palmer Drought Severity Index (PDSI) (Palmer, 1965), the Crop Moisture Index (CMI) (Palmer, 1968), the Normalized Difference Vegetation Index (NDVI) (Rouse et al., 1974), the Standardised Precipitation Index (SPI) (McKee et al., 1993; Ganguli and Reddy, 2014), the Drought Recognition Index (RDI) (Tsakiris and Vangelis, 2005) and the Standardised Precipitation Evapotranspiration Index (SPEI) (Vicente-Serrano et al., 2010). In particular the SPI, despite the inherent limitations, was considered in several studies to investigate drought characteristics across the world (Mishra and Singh, 2010; Van Loon, 2015).

For what concerns the Italian territory, Capra et al. (2012) investigated the spatio-temporal variability of drought at short and medium accumulation scale in the Calabria region, southern of Italy, using the SPI index, concluding that approximately half of the region was impacted by drought during the period 1981-1990, when the region suffered its worst drought. Di Lena et al. (2014) analysed drought periods in the Abruzzo region, showing a general downward trend in SPI time series, more pronounced on longer accumulation time scales. Marini et al. (2019) investigated droughts in Apulia region using the SPI and



the RDI indexes, finding an upward trend in the severity of droughts in the western part and a downward trend in the eastern
60 region. By applying the SPI index over 3 and 6-months for a short term and 12, 24-months for a long term, Caloiero et al.
(2018) analysed dry and wet period in southern Italy, showing that when long-term precipitation scales are included, the
probabilities of occurrence of dry conditions are higher than the wet one.

The reported case study is represented by the Campania region, located in southern Italy, a large area of about 14000 km²,
stretching from the Apennine Mountains to the Mediterranean Sea with a progressively decreasing elevations moving from
65 the inlands to the coastline. The climate regime of the study area is typically seasonal with some evident differences depending
on the location (Longobardi and Villani, 2010; Longobardi and Mautone, 2015; Longobardi et al., 2016; Longobardi and
Boulariah, under review). Two distinct rain gauge networks are available for the region, one for the period 1918-1999 and the
other for the period 2000-2019. They are characterized by different stations consistency, localisation and typology. With the
aim to reconstruct continuous long-term monthly scale precipitation time series, the in-situ point measurements (observed at
70 the rain gauge locations) for the two datasets were projected on a 10 x10 km resolution grid covering the whole region by
using a geostatistical interpolation approach (Boulariah et al., 2020). Projecting the two distinct database point measurements
to a common grid, made it possible the reconstruction of centennial historical time series of monthly precipitation time series
from 1918-2019 crucial for long term historical drought conditions analysis.

The reconstructed gridded precipitation database was used to compute the Standardized Precipitation Index at different
75 accumulation time steps, from SPI_3 to SPI_48, to explore the full range of drought definitions. SPI time series were analyzed
for their spatial and temporal patterns features and the Modified Mann-Kendall and the Sen's slope test were used to assess
the trend significance and magnitude. Additionally, the spatial patterns of drought characteristics were evaluated with the
assessment of probability of occurrence, drought duration, drought severity and drought peak value, for different SPI
thresholds, according to the run theory (Yevjevich, 1967).

80 The findings of the study in terms of detailed spatial and temporal characterization of drought conditions within the Campania
region, represent an essential information for sustainable and efficient water resources management planning strategies.

2 Material and methods

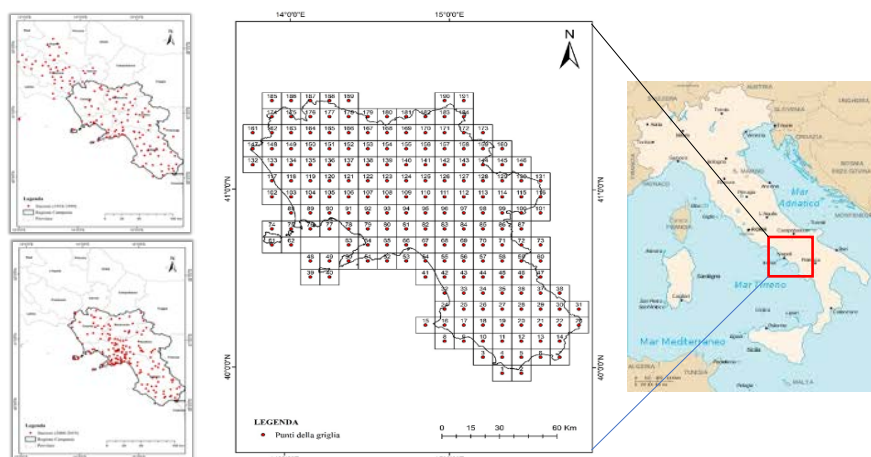
2.1 Study area

The Campania region is located between 40.0 and 41.5° N and 13.5-16.0° E, covering about 14000 km² in southern Italy
85 (Figure 1).

The region is well known for a complex orography; the altitude of the region ranges from well above 2000 m.m.s.l. in the
Apennine Mountains to the coastline. The region is characterized by a complex climatic pattern, because of the orography.
The seasonality is quite marked, with the larger amount of precipitation recorded during the winter periods. The mean annual
rainfall of the study area ranges from 600 to 2400 mm whereas the average annual temperature is around 17°C. Trend in
90 historical precipitation and their seasonal variability were described in Longobardi and Villani (2010) and Longobardi et al.



(2016). The area is experiencing a moderate negative trend in precipitation, especially for what concerns the north-east and south-west areas. At the same time, also the seasonal variability appeared to be featured by a negative trend, with a transition of the precipitation regime from a seasonal to more uniform one.



95 **Figure 1: The studied area. Left panel: the two rain gauges dataset. Middle panel: the grid shape for the region under investigation. Precipitation data are referred to the centre of each cell. Right panel: the Italian peninsula.**

2.2 Dataset

As mentioned in the introduction, the gridded datasets used in the current paper was obtained from the research carried out by Boulariah et al. (2020), where different spatial interpolation approaches (both deterministic and geostatistical approaches), were applied to merge two monthly precipitation rain gauge (point) database available for the studied region, as they are
100 different in rain gauge locations and moreover cover different periods of time, being one referred to the period 1918-1999 and the second to 2000-2019 (Figure 1 left panel). The two-point dataset (rain gauges dataset) were spatially interpolated by the cokriging, which was found to be the best interpolating method over the investigated area based on the results of an interpolation approaches comparative study, due to the high correlation ($\geq 70\%$) between elevation and observed precipitation (Boulariah et al., 2020). The interpolated precipitation field (for each month and for each year) were projected on a high-
105 resolution grid base ($0.09^\circ \times 0.09^\circ$, 10 x 10 km). The result of the merging process was monthly gridded rainfall data from 1918 to 2019 for 191 high resolution grid points covering the whole of the Campania region, which were considered for the proposed analysis (Figure 1, middle panel).

2.3 the Standardized Precipitation Index

110 The formulation of the SPI drought index for any given location is based on the cumulative rainfall record over a selected time scale and the probability density function “Gamma” which fit only positive and null values (McKee et al., 1993; Husak et al., 2007). In the literature and according to different previous studies, the rainfall time series are first fitted to the Gamma distribution and then standardized by transformation into a normal distribution (Caloiero et al., 2018; Martinez et al.,



2019;Stagge et al., 2015;Zhou and Liu, 2016). The probability density function for the Gamma distribution can be expressed
 115 by the following equation:

$$g(x) = \frac{1}{\beta^\alpha \Gamma(\alpha)} x^{\alpha-1} e^{-x/\beta} \quad (1)$$

Where α , β and x are respectively the shape parameter, the scale parameter and the amount of precipitation (α , β and $x > 0$).
 $\Gamma(\alpha)$ is the gamma function expressed as:

$$\Gamma(\alpha) = \int_0^\infty y^{\alpha-1} e^{-y} dy \quad (2)$$

120 Parameters $\hat{\alpha}$ and $\hat{\beta}$ are assessed through the maximum likelihood method (McKee et al., 1993;Liu et al., 2016):

$$\hat{\alpha} = \frac{1}{4A} \left(1 + \sqrt{1 + \frac{4A}{3}} \right) \text{ and } \hat{\beta} = \frac{\bar{x}}{\hat{\alpha}} \quad (3)$$

where

$$A = \ln(\bar{x}) - \frac{\sum \ln(x)}{n} \quad (4)$$

for n observations. By integrating the density of probability function $g(x)$, the cumulative probability $G(x)$ is obtained:

125
$$G(x) = \int_0^x g(x) dx = \frac{1}{\hat{\beta} \Gamma(\hat{\alpha})} = \int_0^x x^{\hat{\alpha}-1} e^{-\frac{x}{\hat{\beta}}} dx \quad (5)$$

Given the Gamma distribution is not defined for x values equal to zero and that instead the cumulative rainfall series may
 contain null values, the cumulative distribution is re-defined as follows:

$$H(x) = q + (1-q) G(x) \quad (6)$$

130 where q is the probability of zero precipitation. Then, the value of the SPI can be obtained through the approximation proposed
 in Abramowitz and Stegun (1964) which converts the cumulative distribution $H(x)$ to a normal random variable Z :

$$Z = \text{SPI} = \begin{cases} - \left(t - \frac{c_0 + c_1 t + c_2 t^2}{1 + d_1 t + d_2 t^2 + d_3 t^3} \right), & \text{for } 0 < H(x) \leq 0.5 \\ + \left(t - \frac{c_0 + c_1 t + c_2 t^2}{1 + d_1 t + d_2 t^2 + d_3 t^3} \right), & \text{for } 0.5 < H(x) \leq 1 \end{cases} \quad (7)$$

$$t = \begin{cases} \sqrt{\ln \left[\frac{1}{(H(x))^2} \right]}, & \text{for } 0 < H(x) \leq 0.5 \\ \sqrt{\ln \left[\frac{1}{(1-H(x))^2} \right]}, & \text{for } 0.5 < H(x) \leq 1 \end{cases} \quad (8)$$

where:

135
$$c_0 = 2.515517, c_1 = 0.802853, c_2 = 0.010328$$

$$d_0 = 1.432788, d_1 = 0.189269, d_2 = 0.001308$$



SPI time series for different accumulation periods of 3, 6, 12, 24, 36 and 48 months (respectively SPI_3, SPI_6, SPI_12, SPI_24, SPI_36 and SPI_48) were computed for the studied dataset and used to describe wet and dry conditions according to the following values (McKee et al., 1993):

SPI Values	Drought severity
$SPI \geq 2.0$	Extremely wet
$1.5 \leq SPI < 2.0$	Very wet
$1.0 \leq SPI < 1.5$	Moderately wet
$-1.0 < SPI < 1.0$	Near normal
$-1.5 < SPI \leq -1.0$	Moderately dry
$-2.0 < SPI \leq -1.5$	Severely dry
$SPI < -2.0$	Extremely dry

140 **Table 1: classification of wet and dry conditions according to SPI values (Mc Kee et al., 1993).**

2.4 Trend analysis

Time series of SPI were tested for trend detection in time. A trend is a significant change over time exhibited by a random variable, detectable by statistical parametric and non-parametric procedures. Provided the intrinsic autocorrelation of the analyzed time series, the current study provided results for non-parametric Modified Mann-Kendall (MMK) and Sen's tests approaches. Those methods are briefly described in the following.

The Mann-Kendall test (Mann, 1945; Kendall, 1948) is one of the most widely used methods to detect trend in climatology analysis. It is used to analyze data collected over time for consistently increasing or decreasing trends (monotonic). It is a non-parametric test, which means it works for all distributions, thus tested data does not have to meet the assumption of normality but should have no serial correlation. The Mann-Kendall statistic S is defined as:

$$S = \sum_{i=1}^{n-1} \sum_{j=i+1}^n \text{sign}(x_j - x_i) \quad (9)$$

where:

$$\text{sign}(x_j - x_i) = \begin{cases} +1, & \text{if } (x_j - x_i) > 0 \\ 0, & \text{if } (x_j - x_i) = 0 \\ -1, & \text{if } (x_j - x_i) < 0 \end{cases} \quad (10)$$

x_i and x_j are the annual values in years i and j , with $i > j$. When $n \geq 10$, the statistic S is almost normally distributed with mean E(S) and variance Var(S) as follows:

$$E(S) = 0, \quad \text{Var}(S) = \frac{n(n-1)(2n+5)}{18} \quad (11)$$

however, the expression of Var(S) should be adjusted when tied value do exist:



$$Var(S) = \frac{1}{18} \left[n(n-1)(2n+5) - \sum_{p=1}^q t_p(t_p-1)(2t_p+5) \right] \quad (12)$$

where q is the number of tied groups and t_p is the number of data values in the p -th group. The standardized test statistic Z follows a standard normal distribution and is computed as follows:

$$Z = \begin{cases} \frac{S-1}{\sqrt{Var(S)}} & \text{if } S > 0 \\ 0 & \text{if } S = 0 \\ \frac{S+1}{\sqrt{Var(S)}} & \text{if } S < 0 \end{cases} \quad (13)$$

At the significance level α , the existing trend is considered to be statistically significant if $p \leq \alpha/2$ in the case of the two-tailed test.

To take account of the presence of autocorrelation in the SPI time series, which might increase the probability to detect trends when actually none exists, the Modified Mann-Kendall test can be applied (Hamed and Rao, 1998). For this purpose, a modified form of $Var(S)$, set as $Var(S)^*$, is used as follows:

$$Var(S)^* = Var(S) \frac{n}{n^*} \quad (14)$$

where n^* is the effective sample size and n the number of observations. The ratio between the effective sample size and the actual number of observations was computed as proposed by (Hamed and Rao, 1998) as follows:

$$\frac{n}{n^*} = 1 + \frac{2}{n(n-1)(n-2)} \sum_{i=1}^{n-1} (n-i)(n-i-1)(n-i-2)r_i \quad (15)$$

where: r_i is the lag- i significant auto-correlation coefficient of rank i of time series.

Sen (1968) developed a non-parametric procedure to assess the slope of trend in a sample of N pairs of data:

$$T_i = \frac{x_j - x_i}{j - i}, \quad i = 1, 2, \dots, N, \quad j > i \quad (16)$$

where x_j and x_i are data values at time j and i ($j > i$) respectively. The Sen's estimator of slope is defined by the median of the N values of T_i :

$$T = \begin{cases} \frac{Q_{N+1}}{2} & \text{if } N \text{ is odd} \\ \frac{1}{2} \left[\frac{Q_N}{2} + \frac{Q_{N+2}}{2} \right] & \text{if } N \text{ is even} \end{cases} \quad (17)$$

The T sign reflects the data trend behavior (increase or decrease), while its value indicates the steepness of the trend.

2.5 Drought characteristics

To describe droughts features of the studied area, in a first step the occurrence of drought events, according to a given SPI threshold, was evaluated for each cell of the gridded dataset and the average over the period of observation was illustrated.

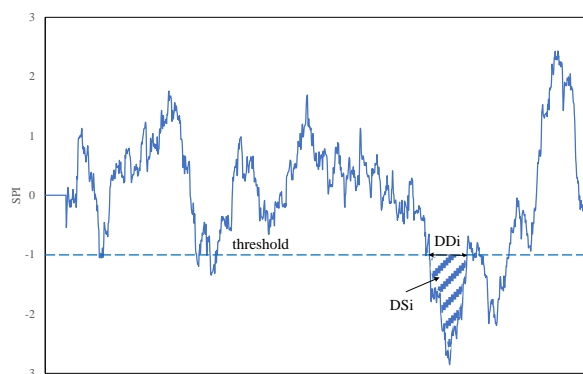


Two different thresholds in the SPI value were used, $SPI \leq -1$ and $SPI \leq -2$, to detect the behavior of the region with respect to moderate and extremely severe drought conditions (see Table 1). The effect of the accumulation period was investigated. Additionally, three drought characteristics, namely mean drought duration (MDD), mean drought severity (MDS) and mean drought intensity (MDP) (Guo et al., 2018; Wang et al., 2019; Fung et al., 2020) were selected. By linking the SPI data with the “run theory” proposed by (Yevjevich, 1967), and according to (Wang et al., 2019) MDD and MDS were calculated as follows:

$$MDD = \frac{\sum_{i=1}^N DD_i}{N} \quad (18)$$

$$MDS = \frac{\sum_{i=1}^N DS_i}{N}, DS = \sum_{DD} \text{Drought Index Value}, DS < 0 \quad (14)$$

where N is the number of drought spells observed during the studied period, DD is the period with continuous negative values of the drought index, i is the number of months with negative values of the drought index, DS is the value of drought severity (Figure 2). Events with $DD \geq 3$ months were only accounted for. Additionally, the mean drought intensity MDP was computed as the ratio between MDS and MDD (Li et al., 2017). As in the case of the computation of MDD, MDS and MDP, the two different thresholds, $SPI \leq -1$ and $SPI \leq -2$, were taken into consideration. The effect of the accumulation scale and the spatial patterns were investigated.



195 **Figure 2. Drought characteristics identification using the ‘run theory’ (Yevjevich 1967).**

3. Results and discussion

3.1 Temporal analysis

The temporal patterns of the SPI time series in the region under investigation at different time scales have the potential to provide insights into the temporal variation of droughts in the Campania. As an example, Figure 3 illustrates SPI₆, SPI₁₂ and SPI₂₄ for two cells of the grid data (Figure 1). In the left panel an example from the southern coastal area is depicted whereas in the right panel an example from the northern inland area.

In both areas, Figure 3 clearly highlights the drought periods that affected the Campania region around the 1940-1950 and around 1990-2010. Even though drought severity appears almost the same within the two cells, looking at the longest accumulation time scale, it is clear how drought tends to be more persistent in the inland areas, which additionally have not



been strongly impacted by the drought conditions started in the 2015 in the region. More details about the spatial variability of drought features will be discussed in the following.

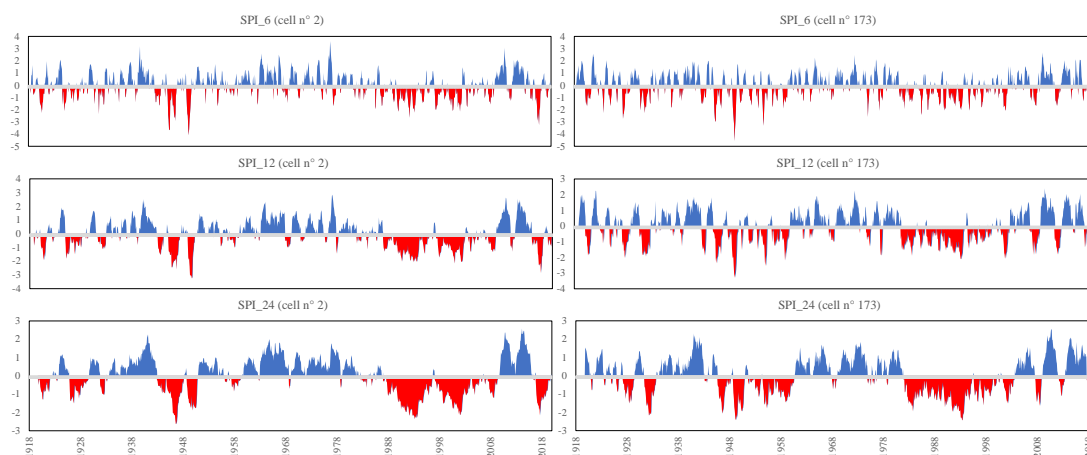
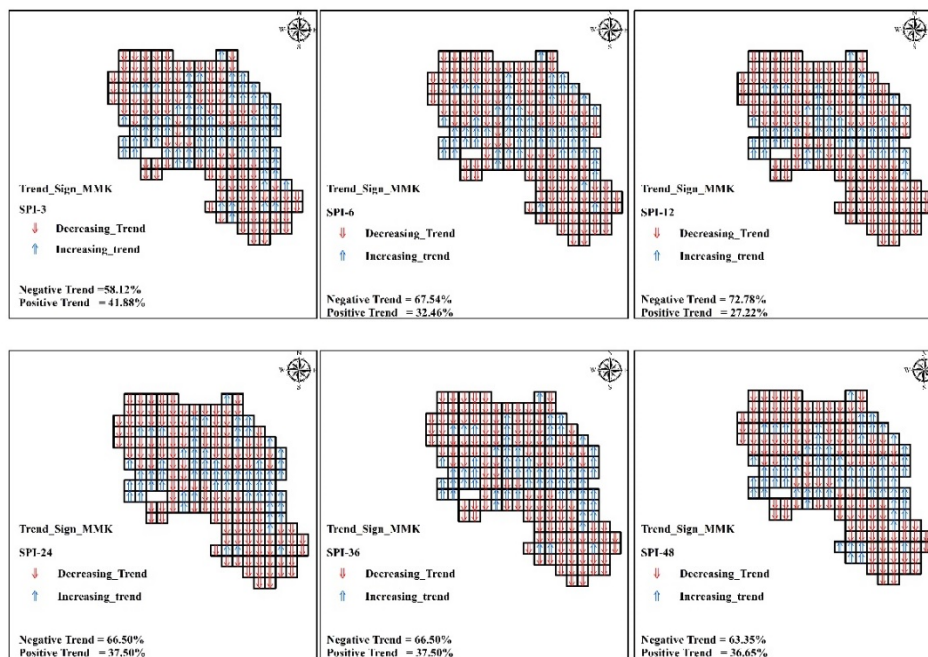


Figure 3. SPI_6, SPI_12 and SPI_24 for cell n°2 (southern area – left panel) and cell n° 173 (northern area – right area).

210 The Modified Mann-Kendall (MMK) trend tests and the Sen's slope estimator were carried out to investigate temporal trends, sign, significance and magnitude in SPI time series over the studied period. The reason for the use the Modified Mann-Kendal test (MMK) lays in its accuracy for the analysis of correlated data (Hamed and Rao, 1998; Mondal et al., 2012; Sa'adi et al., 2019), which is the case for the SPI time series in this study, compared to the original Mann-Kendall trend test without any loss of power. The relevant results of the Modified Mann-Kendall Test (MMK) for trend sign and significance (significance level = 5%) are shown respectively in Figure 4 and Figure 5.



215 **Figure 4: SPI MMK test sign, for the different accumulation scales ($\alpha = 5\%$).**

Starting from the SPI_3 to SPI_12, the downward trend become dominant in the study area and especially marked in the northwest and south sectors of the region, featured by the largest Precipitation Concentration Index, that is the area with the more relevant climate seasonality in the region (Longobardi et al., 2016). The proportion of negative to positive trend, with negative values still dominant in over 60% of the cells, remains almost similar for the SPI_24 to SPI_48.

For what concern the significance of the trend, the MMK test illustrated how a very large proportion of the gridded SPI showed a significant trend over the different time scales especially from the SPI_3 to the SPI_24 accumulation scale (Figure 5). For the SPI_3, SPI_6 and SPI_12, the negative trend is particularly significant, with a percentage of grid cells of about 55% for both SPI_3 and SPI_6 and 65% for SPI_12. Regarding the spatial distribution of the trend, the SPI_24 is the most significant with almost 70% of the grid cells. On the national scale the obtained results were well in line with the general overview outlined in a previous research by Delitala et al. (2000) and Bordi et al. (2001) for other regions of southern Italy (Sardinia, Sicily and Puglia) and, furthermore, were in perfect accord with the outcomes given by Buttafuoco and Caloiero (2014) for the Calabria region in southern Italy.

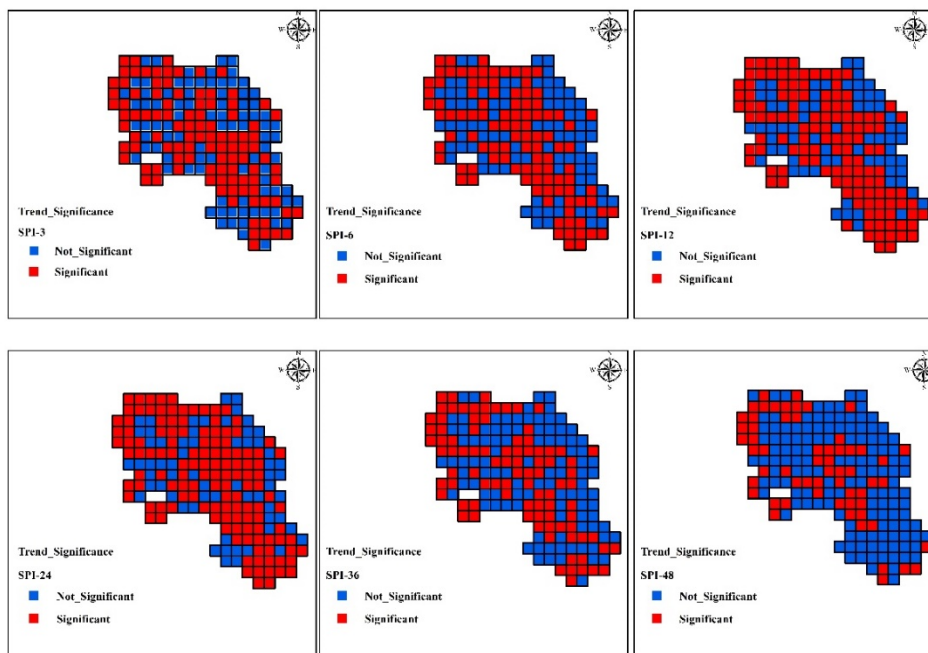


Figure 5: SPI MMK test significance ($\alpha = 5\%$), for the different accumulation scales.

230 The magnitude of the trend in the SPI time series, as assessed using Sen's estimator, is presented in Figure 6. In agreement
with the results of the MKK test, the trend was dominantly negative across the region, with some exception for a wet-east
transect at the middle latitude of the region. On average, the tendency toward drier conditions was however rather moderate
and characterized by an amplification with increasing accumulation time scale. The increase in the SPI index amount to about
10%, in ten years for the case of SPI_6. It increases up to 15% to 24%, in ten years, respectively for the case of SPI_12 and
235 SPI_48. The variability in the minimum and maximum assessed trend, on the spatial scale, also increases for increasing
accumulation time scale.

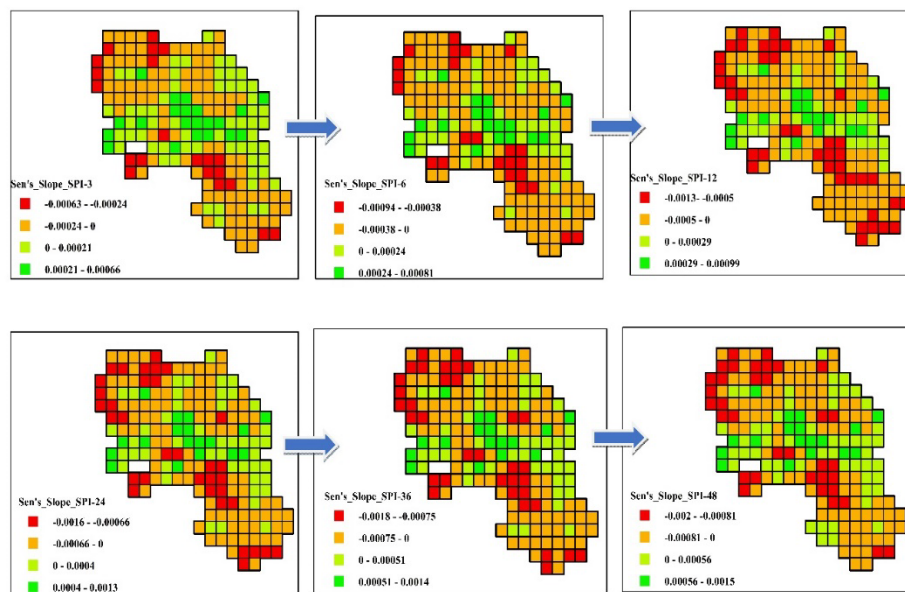


Figure 6: SPI Sen's slope, for the different accumulation time scales.

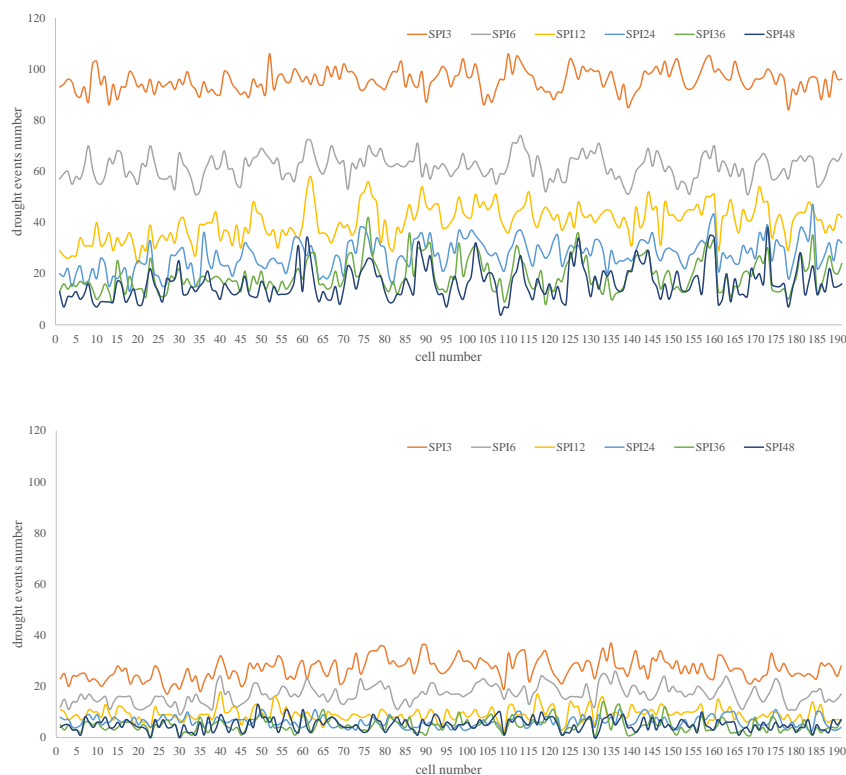
3.2 Drought characteristics

240 Figure 7 shows the total number of drought events detected within the SPI time series from 1918 to 2019 for moderate drought conditions (threshold $SPI \leq -1$) and for extremely severe drought conditions (threshold $SPI \leq -2$) for each point of the grid for all the accumulation scales considered. In the case of moderate drought events, it was observed that the SPI_3 is associated to the largest number of droughts, which was on average 95, for the whole period of observation, over the 191 grid cells. Provided the large theoretical autocorrelation in SPI timeseries for the larger accumulation scale, drought frequency decreased

245 with increasing accumulation scale, with the SPI_24 to SPI_48 patterns almost similar among them (Figure 7 upper panel). The results appeared in good agreement with what demonstrated by other authors (McKee et al., 1993; Buttafuoco et al., 2015; Marini et al., 2019; Fung et al., 2020). A very similar behavior was found in the case of extremely severe droughts episodes, unless for the lower number compared to the case of moderate events. The average number of drought events in the case of SPI_3 for the threshold $SPI \leq -2$, was on average 27, for the whole period of observation, over the 191 grid cells. For

250 what concerns the spatial patterns, although a moderate correlation appeared for small cluster of cells, it was not found an evident concentration of drought events occurrence in a specific area.

More insights came from the analysis of the MDD, MDS and MDP, respectively illustrated in Figure 8, 9 and 10 with reference to a threshold value of $SPI \leq -1$.



255 **Figure 7: Drought event numbers, for the different accumulation time scales, over the whole period of observation 1918-2019. Upper panel: moderate drought events ($SPI \leq -1$). Lower panel: extremely severe drought events ($SPI \leq -2$)**

For what concerns the MDD, differently from what occurred in terms of drought frequency, the mean drought duration increased with the accumulation time scale, ranging from 4 to 5 months for the SPI_3, to 8 to 60 months for the SPI_48. The accumulation time scale also affected the MDD spatial behaviour (Figure 8). In the case of SPI_3 and SPI_6, almost the whole region was affected by the average MDD values. In the case of SPI_12, SPI_24, SPI_36 and SPI_48, the largest MDD values were detected along a north-west to south-east transect and however more evidently in the southern sectors of the region. The maximum values detected in the southern region for the larger accumulation time scale were mainly caused by severe drought periods occurred in the '90, 2003 and 2017 in the region.

For what concerned the MDS, because of the MDD characteristics, the drought severity increased with the accumulation time scale ranging from 6 to 8 for the SPI_3, to 11 to 90 for the SPI_48 (Figure 9). The spatial pattern of MDS was affected by the accumulation time scale, such as in the case of the MDD. For the SPI_3 to SPI_6, MDS showed a broad variability over the investigated area, whereas moving from SPI_12 to SPI_48, MDS appeared evenly distributed and set on an almost constant value (about -10), with an exception for a north-west to south-east transect and however for the southern sectors of the region where the largest MDS values were detected.



270 For what concerned the MDP, because of what previously observed in the case of the MDD and MDS, the minimum (about -
1.5 on average) and maximum (about -2.3 on average) values appeared similar for the different accumulation time scale, likely
more pronounced for the lower accumulation scales. Differently, the spatial pattern was found to be particularly complex and
did not show a clear tendency related to the accumulation time scale (Figure 10). Overall, the largest peaks are detected in the
northern areas of the region for the SPI_3 to SPI_6. From SPI_24 to SPI_48 there was a general tendency for a dominant low
275 peak spatial distribution, with an exception for some coastline areas in the north of the region. The SPI_12 represented a neutral
condition, with a very important spatial variability of peak conditions.

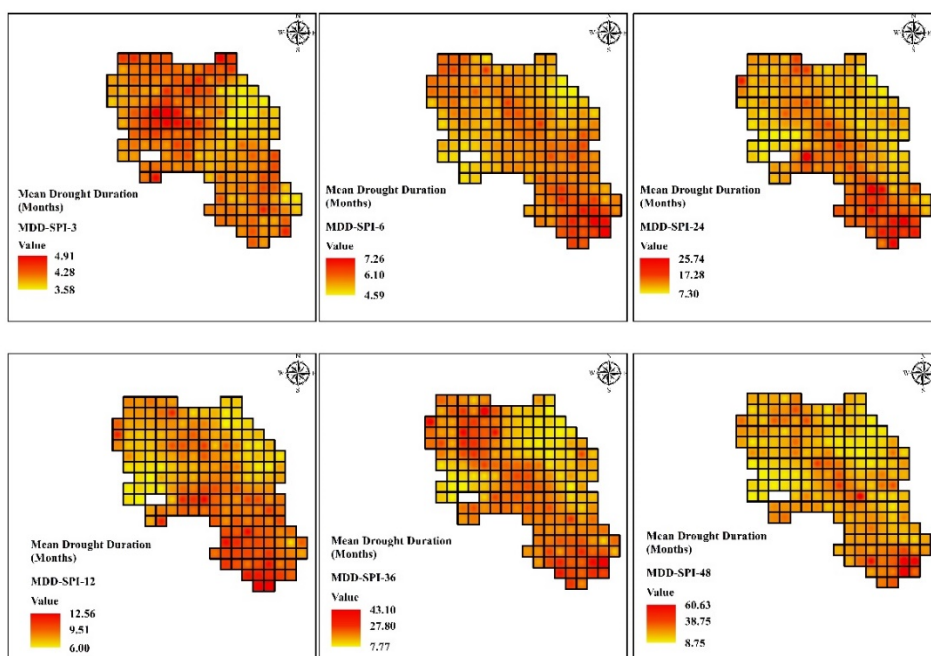


Figure 8: MDD (mean drought duration) for the different considered accumulation periods (SPI ≤ -1).

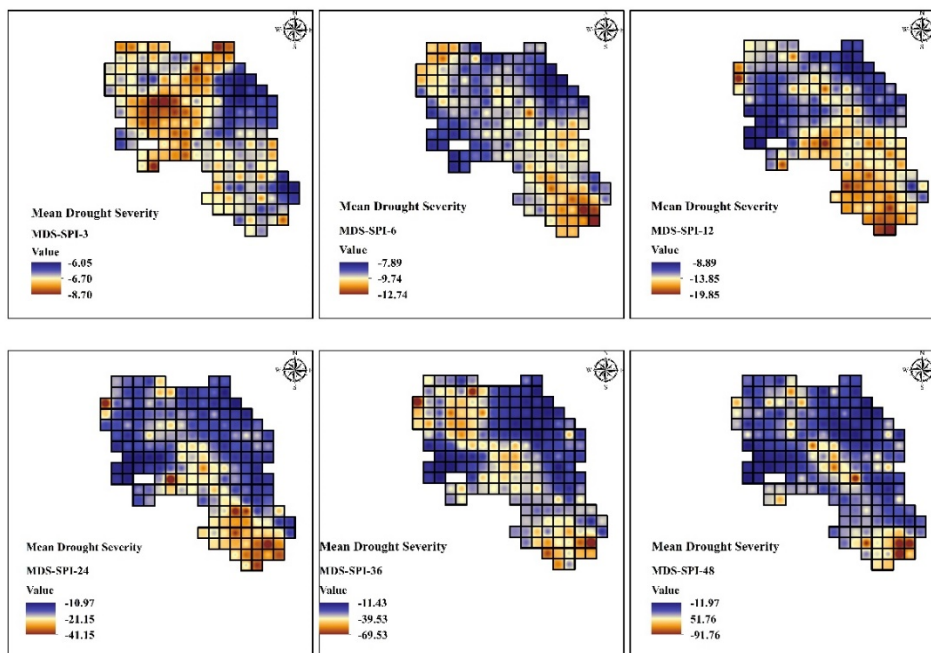


Figure 9: MDS (mean drought severity) for the different considered accumulation periods ($SPI \leq -1$).

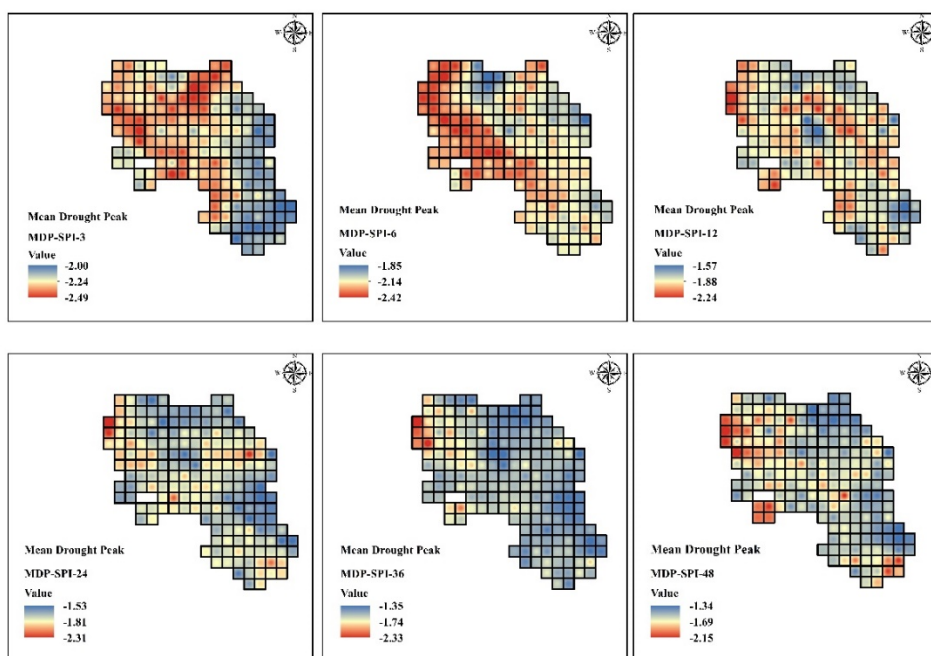


Figure 10: MDP (mean drought peak) for the different considered accumulation periods ($SPI \leq -1$).



280 By increasing the threshold for the SPI values, moving from $SPI \leq -1$ to $SPI \leq -2$, it was possible to explore the extremely severe drought conditions over the region.

For what concerned the MDD (Figure 11), the mean drought duration increased with the accumulation time scale, ranging from 3 months for the SPI_3, to 47 months for the SPI_48. Compared to the case of moderate drought events, in the case of extremely severe events the mean drought duration decreased for each accumulation scale. For what concerned the spatial distribution, 285 the same consideration provided for the case of SPI threshold ≤ -1 hold also in the case of SPI threshold ≤ -2 .

With reference to the MDS, accordingly to the MDD, the drought severity increased with the accumulation time scale ranging from 16 for the SPI_3, to 109 for the SPI_48 (Figure 12). Compared to the case of moderate drought events, in the case of extremely severe events the mean drought severity increased for each accumulation scale. For what concerned the spatial pattern of MDS, it appeared a common feature according to which the largest MDS values appeared in the central area of the 290 region, with some spot cells located in the extremely southern and extremely northern coastline. An exception was provided by the lower SPI_3.

In the end, for what concerned the MDP, differently to what occurred in the case of the MDD and MDS, the minimum (about -2.5 on average) and maximum (about -3.5 on average) values appeared similar for the different accumulation time scale, likely more pronounced for the lower accumulation scales (-4.09 for SPI_6). The spatial pattern was found to be particularly 295 complex and did not show a clear tendency related to the accumulation time scale (Figure 13). Larger peaks were still focused in the central area of the region, but the area covered changed with accumulation time scale, being rather moderate for the larger SPI accumulation scale. Large peak appeared to spread all over the region in the case of the largest accumulation periods, for SPI_36 and SPI_48.

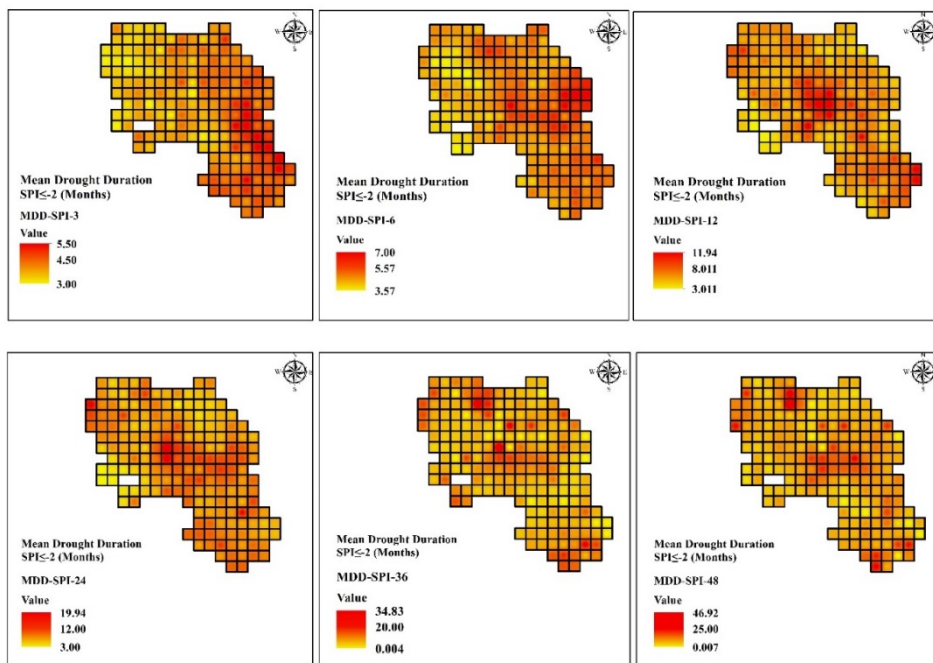
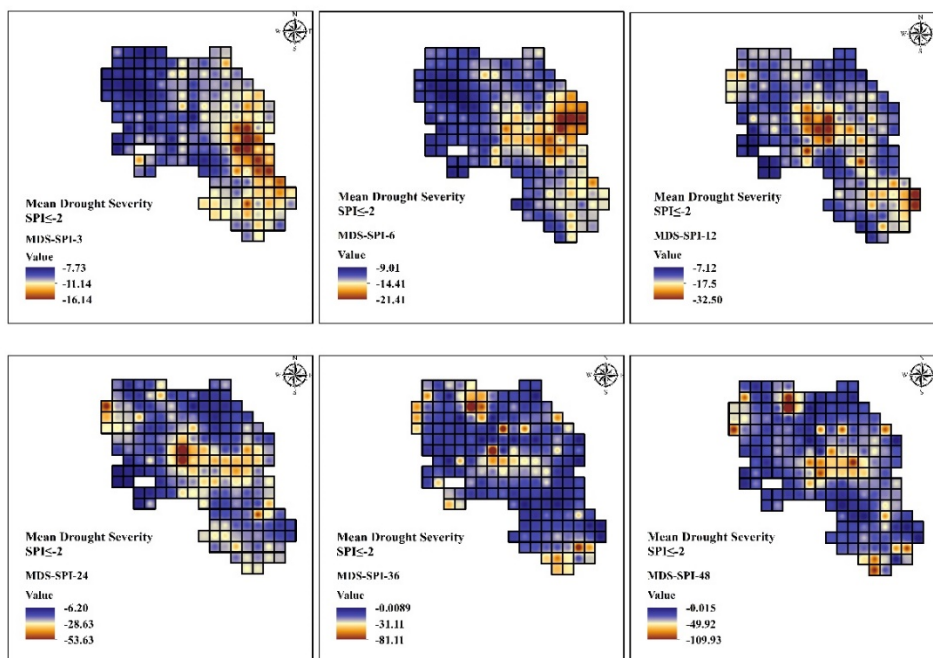


Figure 11: MDD (mean drought duration) for the different considered accumulation periods (SPI ≤ -2).



300 Figure 12: MDS (mean drought severity) for the different considered accumulation periods (SPI ≤ -2).

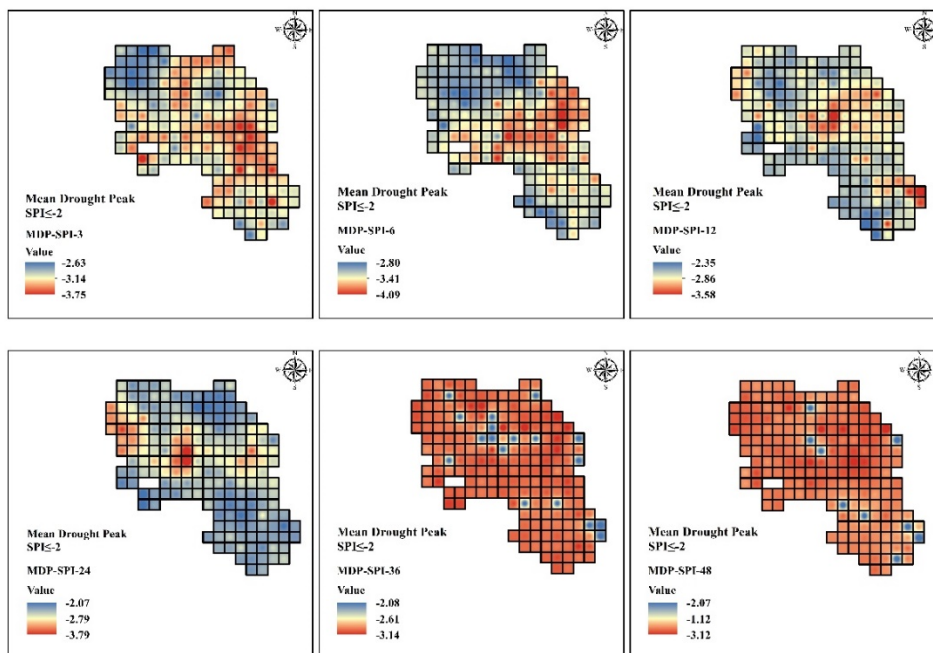


Figure 13: MDP (mean drought peak) for the different considered accumulation periods ($SPI \leq -2$).

4. Conclusions

Drought is a sustained period of below-normal water availability. It is a recurring and worldwide phenomenon, but the Mediterranean basin is seen as a very vulnerable environment in this perspective. The main objective of this study was to assess the drought features in the Campania region of southern Italy through an analysis of the spatial and temporal patterns characteristics of SPI time series, computed at different accumulation scales, over a centennial period, from 1918 to 2019. The Modified Man Kendal test and the Sen's test were applied to describe the temporal trend significance and magnitude. Additionally, for both moderate ($SPI \leq -1$) and extremely severe ($SPI \leq -2$) drought conditions, the “run theory” (Yevjevich 1967) was applied to illustrate drought events frequency, duration, peak and severity.

For what concerns the drought temporal features, the trend was found to be dominantly negative and to increase with accumulation scale. It remained almost similar for SPI time series computed over 24 months or larger intervals. The significance was also found to be particularly evident approaching 70% of grid cells for SPI₂₄. The SPI increase over time ranged from about 10%, in ten years, for the case of SPI₆ to 24%, in ten years, for the case of SPI₄₈. In the case of moderate dry conditions, MDD increased with the accumulation time scale, ranging from about 5 months for the SPI₆, to 60 months for the SPI₄₈. Accordingly, MDS increased with accumulation scale, moving from about -10 in the case of SPI₆ to about -50 in the case of SPI₄₈. MDP did not changed significantly with the accumulation scale and was particularly pronounced in



the case of the lower temporal scales. Extremely severe events were featured by lower durations and larger severity compared to the moderate drought events but were very less frequent (over 75% less then).

320 For what concerned the spatial pattern, the negative trends appeared to occur along a north-west to south-east transect, whereas positive trend were focused along a west-east transect at the middle latitude of the region. The accumulation time scale affected the MDD spatial behavior as almost the whole region was affected by similar average MDD values for small time scales whereas large MDD values were detected along a north-west to south-east transect and however more evidently in the southern sectors of the region. The maximum values detected in the southern area for the larger accumulation time scale were mainly

325 caused by severe drought periods occurred in the '90, 2003 and 2017 in the region. MDS spatial pattern was also affected by accumulation scale. It showed a broad variability over the investigated area for the lower temporal scales and instead a constant spatial distribution for the larger temporal scales, with an exception for a north-west to south-east transect and however for the southern sectors of the region where the largest MDS values were detected. In the end, the MDP spatial pattern was found to be particularly complex and did not show a clear tendency related to the accumulation time scale.

330 The reported research illustrated how historical in-situ long term measurements are crucial for understanding historical drought conditions to plan mitigation strategies to further face future climate change impacts.

Author contribution: AL and PV contributed to the conceptualization. AL and OB contributed to data curation and formal analysis. AL and PV provided supervision and AL and OB to the writing of the original draft.

335 **Competing interests:** The authors declare that they have no conflict of interest.

References

- 340 Abramowitz, M., and Stegun, I. A.: Handbook of mathematical functions with formulas, graphs, and mathematical tables, US Government printing office, 1964.
- Bonaccorso, B., Aronica, G.T.: Estimating Temporal Changes in Extreme Rainfall in Sicily Region (Italy), *Water Resour Manag*, 30 (15), 5651-5670, 2016.
- 345 Bordi, I., Frigio, S., Parenti, P., Speranza, A., and Sutera,: The analysis of the Standardized Precipitation Index in the Mediterranean area: regional patterns, *ANN GEOPHYS-ITALY.*, 44, 2001.
- Boulariah, O., Longobardi, A., Nobile, V., Sessa, M. and Villani, P.: Long term monthly precipitation database reconstruction for drought assessment. In: "ClimRisk2020: Time for Action! Raising the ambition of climate action in the age of global emergencies" – SISC Seventh Annual Conference, 21-23 October 2020, 2020.
- Buttafuoco, G., and Caloiero,: Drought events at different timescales in southern Italy (Calabria), *J MAPS.*, 10, 529-537, 2014.
- 350 Buttafuoco, G., Caloiero, T., and Coscarelli, R.: Analyses of drought events in Calabria (southern Italy) using standardized precipitation index, *WATER RESOUR MANAG.*, 29, 557-573, 2015.
- Caloiero, T., Veltri, S., Caloiero, P., and Frustaci, F.: Drought analysis in Europe and in the Mediterranean basin using the standardized precipitation index, *Water.*, 10, 1043, 2018.



- 355 Caloiero, T., Veltri, S., A.: Drought assessment in the Sardinia Region (Italy) during 1922–2011 using the standardized precipitation index, *J APPL GEOPHYS.*, 176, 925-935, 2019.
- Capra, A., Scicolone, B., a: Spatiotemporal variability of drought on a short–medium time scale in the Calabria Region (Southern Italy), *Theor. Appl. Climatol.*, 110, 471-488, 2012.
- Cook, B. I., Anchukaitis, K. J., Touchan, R., Meko, D. M., and Cook, E. R.: Spatiotemporal drought variability in the Mediterranean over the last 900 years, *J. Geophys. Res. Atmos.*, 121, 2060-2074, 2016.
- 360 Delitala, A. M., Cesari, D., Chessa, P. A., and Ward, M. N.: Precipitation over Sardinia (Italy) during the 1946–1993 rainy seasons and associated large-scale climate variations, *INT J CLIMATOL.*, 20, 519-541, 2000.
- Di Lena, B., Vergni, L., Antenucci, F., Todisco, F., Mannocchi, F.: Analysis of drought in the region of Abruzzo (Central Italy) by the Standardized Precipitation Index, *Theor. Appl. Climatol.* 115, 41-52, 2014.
- Dracup, J. A., Lee, K. S., and Paulson Jr, E. G.: On the definition of droughts, *Water Resour. Res.*, 16, 297-302, 1980.
- 365 European drought center., <http://europeandroughtcentre.com/>, last access: 10 December 2020.
- Fung, K., Huang, Y., and Koo, C.: Assessing drought conditions through temporal pattern, spatial characteristic and operational accuracy indicated by SPI and SPEI: case analysis for Peninsular Malaysia, *NAT HAZARDS.*, 103, 2071-2101, 2020.
- Ganguli, P., and Reddy, M. J.: Evaluation of trends and multivariate frequency analysis of droughts in three meteorological subdivisions of western India, *INT J CLIMATOL.*, 34, 911-928, 2014.
- 370 Gouveia, C., Trigo, R. M., Beguería, S., Vicente-Serrano, S. M.: Drought impacts on vegetation activity in the Mediterranean region: An assessment using remote sensing data and multi-scale drought indicators, *GLOBAL PLANET CHANGE.*, 151, 15-27, 2017.
- Guo, H., Bao, A., Liu, T., Ndayisaba, F., Jiang, L., Kurban, A., and De Maeyer, P.: Spatial and temporal characteristics of droughts in Central Asia during 1966–2015, *SCI TOTAL ENVIRON.*, 624, 1523-1538, 2018.
- 375 Hamed, K. H., and Rao, A. R.: A modified Mann-Kendall trend test for autocorrelated data, *J HYDROL.*, 204, 182-196, 1998.
- Hasegawa, A., Gusyev, M., and Iwami, Y.: Meteorological drought and flood assessment using the comparative SPI approach in Asia under climate change, *J. Disaster Res.*, 11, 1082-1090, 2016.
- Husak, G. J., Michaelsen, J., and Funk, C.: Use of the gamma distribution to represent monthly rainfall in Africa for drought monitoring applications, *INT J CLIMATOL.*, 27, 935-944, 2007.
- 380 Kendall, M. G.: Rank correlation methods, 1948.
- LI, X.-X., JU, H., Sarah, G., YAN, C.-R., Batchelor, W.D., LIU, Q.: Spatiotemporal variation of drought characteristics in the Huang-Huai-Hai Plain, China under the climate change scenario, *J. Integr. Agr.*, 16 (10), 2308-2322, 2017.
- Littell, J. S., Peterson, D. L., Riley, K. L., Liu, Y., and Luce, C. H.: A review of the relationships between drought and forest fire in the United States, *GLOB CHANGE BIOL.*, 22, 2353-2369, 2016.
- 385 Liu, Z., Wang, Y., Shao, M., Jia, X., and Li, X.: Spatiotemporal analysis of multiscalar drought characteristics across the Loess Plateau of China, *J HYDROL.*, 534, 281-299, 2016.
- Longobardi, A., and Villani, P.: Trend analysis of annual and seasonal rainfall time series in the Mediterranean area, *INT J CLIMATOL.*, 30, 1538-1546, 2010.



- 390 Longobardi, A., and Mautone, M.: Trend analysis of annual and seasonal air temperature time series in southern Italy, in: *Engineering Geology for Society and Territory-Volume 3*, Springer, 501-504, 2015.
- Longobardi, A., Buttafuoco, G., Caloiero, T., Coscarelli, R.: Spatial and temporal distribution of precipitation in a Mediterranean area (southern Italy), *Environ. Earth Sci.*, 75 (3), art. no. 189, 1-20, 2016.
- Longobardi, A., and Van Loon, A. F.: Assessing baseflow index vulnerability to variation in dry spell length for a range of catchment and climate properties, *HYDROL PROCESS.*, 32, 2496-2509, 2018.
- 395 Longobardi, A., and Boulariah, O.: Long term regional changes in inter-annual precipitation variability in a Mediterranean area, *THEOR APPL CLIMATOL*, under review.
- Mann, H. B.: Nonparametric tests against trend, *Econometrica.*, 245-259, 1945.
- Marini, G., Fontana, N., Mishra, A. K.: Investigating drought in Apulia region, Italy using SPI and RDI, *Theor. Appl. Climatol.*, 137, 383-397, 2019.
- 400 Martinez, C., Goddard, L., Kushnir, Y., and Ting, M.: Seasonal climatology and dynamical mechanisms of rainfall in the Caribbean, *Clim.Dynam.*, 53, 825-846, 2019.
- McKee, T. B., Doesken, N. J., and Kleist, J.: The relationship of drought frequency and duration to time scales, in: *Proceedings of the 8th Conference on Applied Climatology*, 179-183, 1993
- Mishra, A. K., and Singh, V. P.: A review of drought concepts, *J HYDROL.*, 391, 202-216, 2010.
- 405 Mondal, A., Kundu, S., Mukhopadhyay, A.: Rainfall trend analysis by Mann-Kendall test: A case study of north-eastern part of Cuttack district, Orissa, *Int. J. Geol. Earth Sci* 2, 70-78, 2012.
- Pachauri, R. K., Allen, M. R., Barros, V. R., Broome, J., Cramer, W., Christ, R., Church, J. A., Clarke, L., Dahe, Q., and Dasgupta, P.: *Climate change 2014: synthesis report. Contribution of Working Groups I, II and III to the fifth assessment report of the Intergovernmental Panel on Climate Change*, Ipcc, 2014.
- 410 Palmer, W. C.: *Meteorological drought*, US Department of Commerce, Weather Bureau, 1965.
- Palmer, W. C.: *Keeping track of crop moisture conditions, nationwide: the new crop moisture index*, 1968.
- Rouse, J., Haas, R. H., Schell, J. A., and Deering, D. W.: *Monitoring vegetation systems in the Great Plains with ERTS*, NASA Spec. Publ. 351, 309, 1974.
- 415 Ruffault, J., Martin-StPaul, N., Pimont, F., Dupuy, J.-L.: How well do meteorological drought indices predict live fuel moisture content (LFMC)? An assessment for wildfire research and operations in Mediterranean ecosystems, *Agric For Meteorol.*, 262, 391-401, 2018.
- Sa'adi, Z., Shahid, S., Ismail, T., Chung, E.-S., Wang, X.-J.: Trends analysis of rainfall and rainfall extremes in Sarawak, Malaysia using modified Mann-Kendall test, *METEOROL ATMOS PHYS.*, 131, 263-277, 2019.
- 420 Sobral, B. S., de Oliveira-Júnior, J. F., de Gois, G., Pereira-Júnior, E. R., de Bodas Terassi, P. M., Muniz-Júnior, J. G. R., Lyra, G. B., and Zeri, M.: Drought characterization for the state of Rio de Janeiro based on the annual SPI index: trends, statistical tests and its relation with ENSO, *Atmos Res.*, 220, 141-154, 2019.
- Spinoni, J., Naumann, G., Vogt, J. V., and Barbosa, P.: The biggest drought events in Europe from 1950 to 2012, *J. Hydrol. Reg. Stud.*, 3, 509-524, 2015.



- 425 Spinoni, J., Barbosa, P., De Jager, A., McCormick, N., Naumann, G., Vogt, J. V., Magni, D., Masante, D., and Mazzeschi, M.: A new global database of meteorological drought events from 1951 to 2016, *J. Hydrol. Reg. Stud.*, 22, 100593, 2019.
- Stagge, J. H., Kohn, I., Tallaksen, L. M., and Stahl, K.: Modeling drought impact occurrence based on meteorological drought indices in Europe, *J HYDROL.*, 530, 37-50, 2015.
- Stagge, J. H., Kingston, D. G., Tallaksen, L. M., and Hannah, D. M.: Observed drought indices show increasing divergence across Europe, *SCI REP-UK* ., 7, 1-10, 2017.
- 430 Swain, S., and Hayhoe, K.: CMIP5 projected changes in spring and summer drought and wet conditions over North America, *Clim.Dynam.*, 44, 2737-2750, 2015.
- Tsakiris, G., and Vangelis, H.: Establishing a drought index incorporating evapotranspiration, *European.water.*, 9, 3-11, 2005.
- Van Loon, A. F.: Hydrological drought explained, *Wiley Interdiscip. Rev. Water* ., 2, 359-392, 2015.
- 435 Vicente-Serrano, S. M., Beguería, S., and López-Moreno, J.: A multiscalar drought index sensitive to global warming: the standardized precipitation evapotranspiration index, *J CLIMATE* ., 23, 1696-1718, 2010.
- Wang, J., Lin, H., Huang, J., Jiang, C., Xie, Y., and Zhou, M.: Variations of drought tendency, frequency, and characteristics and their responses to climate change under CMIP5 RCP scenarios in Huai river basin, China, *Water.*, 11, 2174, 2019.
- Wilhite, D. A., and Glantz, M. H.: Understanding: the drought phenomenon: the role of definitions, *WATER INT* ., 10, 111-120, 1985.
- 440 Yevjevich, V. M.: Objective approach to definitions and investigations of continental hydrologic droughts, An, Colorado State University. Libraries, 1967.
- Yves, T., Koutroulis, A., Samaniego, L., Vicente-Serrano, S. M., Volaire, F., Boone, A., Le Page, M., Llasat, M. C., Albergel, C., and Burak, S.: Challenges for drought assessment in the Mediterranean region under future climate scenarios, *EARTH-SCI REV.*, 103348, 2020.
- 445 Zhang, L., and Zhou, T.: Drought over East Asia: a review, *J CLIMATE.*, 28, 3375-3399, 2015.
- Zhou, H., and Liu, Y.: SPI based meteorological drought assessment over a humid basin: Effects of processing schemes, *Water.*, 8, 373, 2016.